Supplementary information

Diazonium electroreduction: Evidence for a stepwise mechanism

Laure Pichereau,[a] Laure Fillaud,[b] Nikolaos Kostopoulos,[c] Emmanuel Maisonhaute,[b] Thomas Cauchy,[a] Magali Allain,[a] Jean-Marc Noël,[c] Christelle Gautier*[a] and Tony Breton*[a]

[a] Univ Angers, CNRS, MOLTECH-Anjou, SFR MATRIX, F-49000 Angers, France.

[b] Sorbonne Université, CNRS, Laboratoire Interfaces et Systèmes Electrochimiques, 4 Place Jussieu, 75005 Paris, France.

[C] Université Paris Cité, ITODYS, CNRS, F-75013, Paris, France.

Experimental details

Products and electrode treatment

4-nitrobenzenediazonium tetrafluoroborate (4-NBD) and N-terbutyl-alpha-phenylnitrone (PBN) were used as received from Aldrich. Glassy carbon (GC) electrode was obtained from Bioanalytical Systems Inc. (Model MF-2012; diameter 3 mm). For electrolysis, a 1 cm^2 glassy carbon plate, obtained from GoodFellow, was used. All potentials were reported versus $Ag/AgNO_3$ (10 mM) reference electrode. CG electrode and plate surfaces were cleaned by polishing with Buehler 1 and 0.04 µm alumina slurry. After each polishing step the electrode was washed with nanopure water (18.2 MΩ cm) under sonication. Prior and after each electrochemical derivatization, the electrode was sonicated in acetonitrile for 1 minute.

Ultrafast cyclic voltammetry

For ultrafast cyclic voltammetry (UFCV), gold ball ultramicroelectrodes (UME) were prepared by inserting a gold wire (diameter 25 µm) into a pipet. The gold wire was then sealed into the glass with a heating coil, but a small part remained exposed so that it could be melted with a butane flame. By this method, electrodes presenting a reproducible surface state were thus obtained.[1] UFCV measurements were performed on a home-made potentiostat allowing ohmic drop compensation.[2] For improving the conductivity of the solution, all ultrafast experiments were performed in NBD (5mM) dissolved in CH_3CN + 0.30 M NEt_4BF_4.

Spectroelectrochemistry

Real-time spectroelectrochemistry measurements were performed by using an already-described home-made cell.[3] Electrochemical measurements were carried out by using a platinum wire counter electrode and a $Ag/AgNO_3$ (10 mM) reference electrode with a Biologic SP-150 potentiostat driven by EC-Lab software. Experiments were recorded in HPLC-grade acetonitrile with tetrabutylammonium hexafluorophosphate (Bu_4NPF_6, electrochemical grade, Aldrich) as the supporting electrolyte using the following potential program: 30 s at +0.5 V, followed with time by a 15 min electroreduction step at -0.9 V, and a 5 min final step at +0.5 V. Spectrophotometric measurements were carried out in direct reflexing mode on glassy carbon electrode with a home-made bench composed of different Princeton Instruments modules (light sources, fibers, monochromators, spectroscopy camera, and software). The connection between the light source, the cell, and the spectrophotometer is ensured through a "Y-shaped" optical fiber bundle: 18 fibers guide the light to the cell and 19 fibers collect the reflected light from the cell to visible (400–900 nm/maximum acquisition frequency 2 MHz) CCD detector. The sensitivity of the spectroscopic measurement (<3 electrons at 100 kHz and <13 electrons at 2 MHz between 400 and 900 nm) allows a spectroelectrochemistry experiment to be performed under the usual conditions of electrochemistry. For each data set, the reference intensity (I_{ref}) was obtained by averaging the intensity of the first 10 measured frames. Consequently, absorbance variations ($\Delta Abs = -\log_{10}(I/I_{ref})$) and not absorbance values were monitored.

DFT calculations

For all calculations, the Gaussian 09 software (revision D.01) has been used.[4] All ground states in gas phase have been optimized by a DFT approach with the PBE1PBE hybrid functional and the 6–311+G(2d,2p) basis set.[5] A Time Dependent DFT method has been employed to compute the first 15 excited singlet states with the same level of theory. The simulated UV-visible absorption spectra have been obtained by Gaussian broadening of the calculated transition energies (FWHM of 3000 cm^{-1}). Atomic charge mapping has been obtained by Hirshfeld population analysis taking into account interatomic electrostatic interactions. The full molecular reports, molecular orbitals, electron density differences pictures and calculated spectra have been automatically generated by a homemade Python program, quchemreport, based on cclib.[5,6]

Radical scavengering

Electrolysis of 10 mL of 2 mM of 4-NBD and 10 mM of PBN was carried out in a 20 mL 3 electrodes cell during 20 min. The working electrode was a 1 cm^2 classy carbon electrode, the

counter electrode was a Pt grid and the reference electrode was an $Ag/AgNO_3$ (10 mM). After electrolysis, The purification was carried out on silica gel with an acetone/petroleum ether (2:8) eluent to avoid migration nBu_4NPF_6 which migrates from (3:8) into acetone/petroleum ether. Another column on silica gel was necessary with (1:9) then (2:8) acetone/petroleum ether to correctly obtain compounds 1 and 2.

X-ray structure determination

Data collection was performed on a Rigaku Oxford Diffraction SuperNova diffractometer equipped with an Atlas CCD detector and micro-focus Cu-K_α radiation (λ = 1.54184 Å). The structure was solved by dual-space algorithm and refined on F^2 by full matrix least-squares techniques with SHELX programs (SHELXT 2018/2 and SHELXL 2018/3)[7,8] using the WinGX graphical user interface.[9] All non-H atoms were refined anisotropically and multiscan empirical absorption was corrected using CrysAlisPro program (CrysAlisPro 1.171.40.45a, Rigaku Oxford Diffraction, 2019). The H atoms were placed at calculated positions and refined using a riding model. Crystallographic data for the structure have been deposited with the Cambridge Crystallographic Data Centre with the deposition number CCDC 2151044. These data can be obtained free of charge from CCDC, 12 Union road, Cambridge CB2 1EZ, UK (e-mail: deposit@ccdc.cam.ac.uk or http://www.ccdc.cam.ac.uk).

Crystallographic data for LP701: $C_{10}H_{14}N_4O_3$, M = 238.25, orange prism, 0.239 x 0.064 x 0.046 mm, monoclinic, space group $P2_1/n$, a = 6.1119(2) Å, b = 21.6165(8) Å, c = 8.9488(3) Å, β = 96.703(3)°, V = 1174.21(7) $Å^3$, Z = 4, ρcalc = 1.348 g/cm^3, μ = 0.856 mm^{-1}, F(000) = 504, θmin = 4.090°, θmax = 76.229°, 5181 reflections collected, 2409 unique (R_{int} = 0.0131), parameters / restraints = 157 / 0, R1 = 0.0379 and wR2 = 0.1060 using 2179 reflections with I>2σ(I), R1 = 0.0.0418 and wR2 = 0.1101 using all data, GOF = 1.046, -0.219 < $\Delta\rho$ < 0.306 $e.Å^{-3}$.

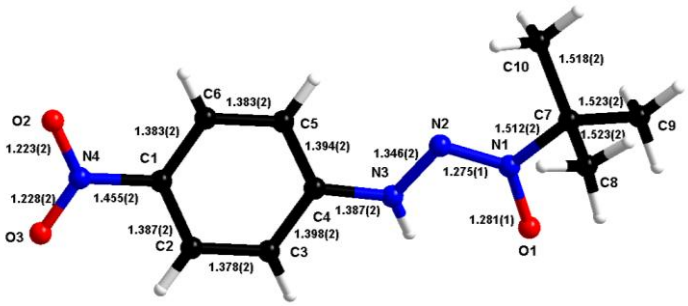

Molecular structure of **LP701** with atomic and bond labels (H atoms omitted for clarity)

Cyclic voltammetry simulations

All the simulations were performed in 1D simulation using the Comsol multiphysics software (edition 5.5). The cyclic voltammetry was simulated as a simple 1-electron process following the classical Butler-Volmer kinetics and following the equation E1.

$$Diazo + 1e^- \rightleftharpoons Diazenyl\bullet \qquad k_{sd} \qquad \text{(E1)}$$

$$Diazenyl\bullet \rightarrow R \qquad k_d \qquad \text{(E2)}$$

The instability of the diazenyl was simulated considering a first order decomposition reaction Equation (E2) with kd, the decomposition rate constant of the diazenyl.

All the parameters used in the simulation are listed in table S1. Noteworthy the real surface of the gold ball UME has not been considered because the absolute current value is not necessary, arbitrary units are used in all the simulated voltamograms.

Table S1. Parameters used for the Simulations of CVs.

Parameter	Value	Definition
a	0.5	
Diazo^0	10^{-3} mol.L^{-1}	Diazonium Concentration
$E_{app,diazo/Diazenyl}$	0.1 V	Apparent redox potential of diazonium
k_{sd}	$3x10^{-2}$ cm.s^{-1}	Heterogeneous ET of the diazonium
D_{diazo}=$D_{diazenyl\bullet}$	$8.14x10^{-6}$ cm^2.s^{-1}	Diffusion coefficient of the diazonium and the diazenyl radical
v	8080 V.s^{-1}	Scan rate

The heterogeneous electron transfer rate constant k_{sd} on gold was extracted by comparing the peak to peak separation potential of the experimental voltammogram in Figure 1b to the simulated ones (k_{sd} = $0.03x10^{-2}$±$0.02x10^{-2}$ cm.s^{-1}) as shown in Figure S1. This value is one order of magnitude higher than the one previously reported on carbon electrode material.[10]

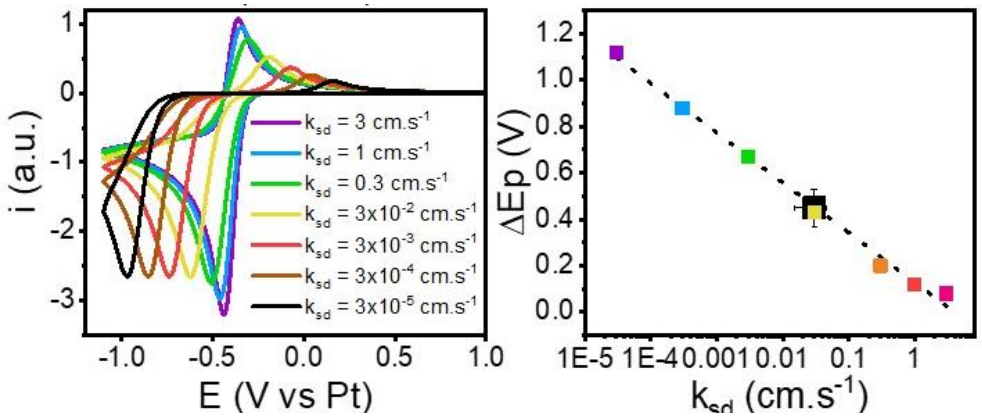

Figure S1. (a) Simulated cyclic voltammograms performed using various heterogeneous electron transfer rate constants, k_{sd} corresponding to the reduction of the diazonium at the electrode. (b) Determination of k_{sd} from the peak to peak separation, ΔEp. The black square corresponds to the experimental ΔEp of Figure 1b and colored ones are determined from ΔEp obtain in (a).

Using those parameters, from the comparison of the intensity ratio i_{ox}/i_{red} obtained experimentally in Figure 1b and the simulated ones (inset Figure 1b and Figure S2a, the dissociation rate constant of Diazenyl• k_d reported in the main text was estimated from Figure S2b.

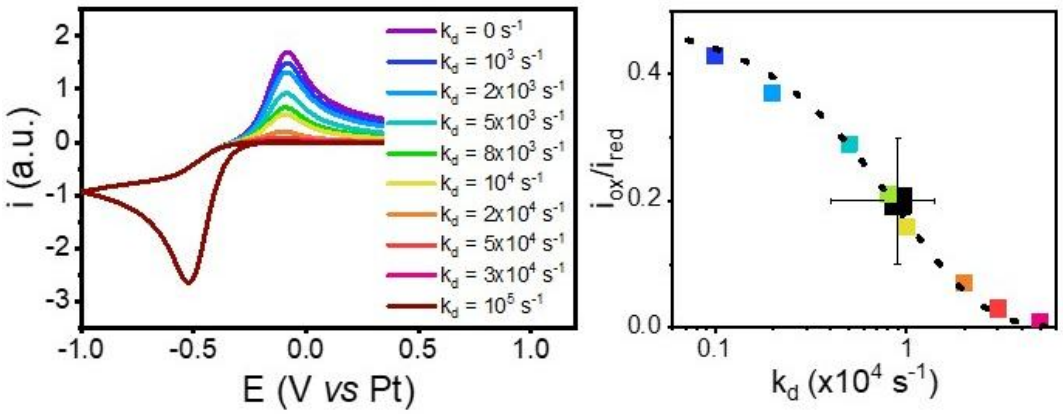

Figure S2. (a) Simulated cyclic voltammograms performed considering various dissociation rate constant of the diazenyl radical, k_d. (b) Determination of k_d from the peak intensity ratio i_{ox}/i_{red}. The black square corresponds to the experimental i_{ox}/i_{red} value extracted from Figure 1b and colored ones are determined from i_{ox}/i_{red} in (a).

Spectroelectrochemistry current-time curves

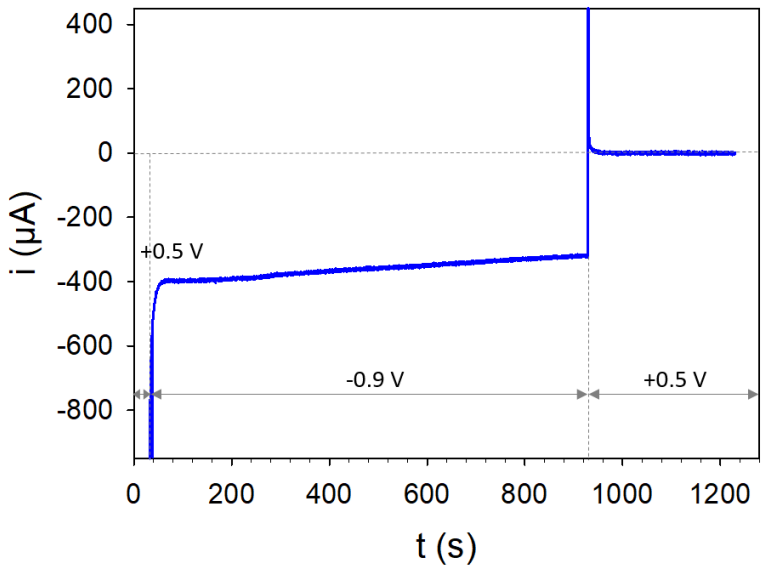

Figure S3. Current-time curves recorded during the A-SEC experiments on glassy carbon in the presence of 1 mM 4-NBD under atmospheric conditions. Potential program: 30 s at +0.5 V, 15 min at -0.9 V and 5 min at +0.5 V.

Spectroelectrochemistry simulations for the diazenyl radical detection

Table S2. Parameters used for the Simulations of the redox inhibitor process.

PARAMETER	VALUE	DEFINITION
a	0.5	
O_2^0	$2x10^{-3}$ mol.L^{-1}	O_2 Concentration
$Diazo^0$	10^{-3} mol.L^{-1}	Diazonium Concentration
E	-0.9 V	Applied Potential
$E_{app,O2/O2^{\bullet-}}$	-0.8 V	Apparent redox potential of O_2
$E_{app,diazo/Diazenyl}$	0.1 V	Apparent redox potential of diazonium
k_f	10^8 $dm^3.mol^{-1}.s^{-1}$	Reaction between $O_2^{\bullet-}$ and diazonium
k_d	10^4 s^{-1}	Instability of diazenyl
k_{sO}	$3x10^{-3}$ cm.s^{-1}	Heterogeneous ET oxygen[10]
k_{sd}	$3x10^{-3}$ cm.s^{-1}	Heterogeneous ET diazonium[10]
$D_{DIAZO}=D_{DIAZENYL^{\bullet}}$	$8.14*10^{-6}$ $cm^2.s^{-1}$	Diffusion coefficient of the diazonium and the diazenyl radical
D_{O2}	$9*10^{-5}$ $cm^2.s^{-1}$	Diffusion coefficient of O_2[11]
$D_{O2^{\bullet-}}$	$2*10^{-5}$ $cm^2.s^{-1}$	Diffusion coefficient of $O_2^{\bullet-}$[11]

As shown in Figure S4a, that plots every 0.1s the concentration profil of the diazenyl radical ($C_{diazenyl^{\bullet}}$) with the distance from the electrode (d), at each time, Diazenyl• exists only in a narrow space (~4µm thickness) within the electrode diffusion layer. Since the light cross the diffusion layer of the electrode perpendicularly, the spectroelectrochemical signal recorded will be proportional to the area corresponding of the presence of Diazenyl• ($\Gamma_{Diazenyl^{\bullet}}$) at each time determined by the simulation. The chronoabsorptogram of Figure 2c presents an increase of Δabs with time followed by a plateau, whereas $\Gamma_{Diazenyl^{\bullet}}$ progressively decreases shown in Figure S4b.

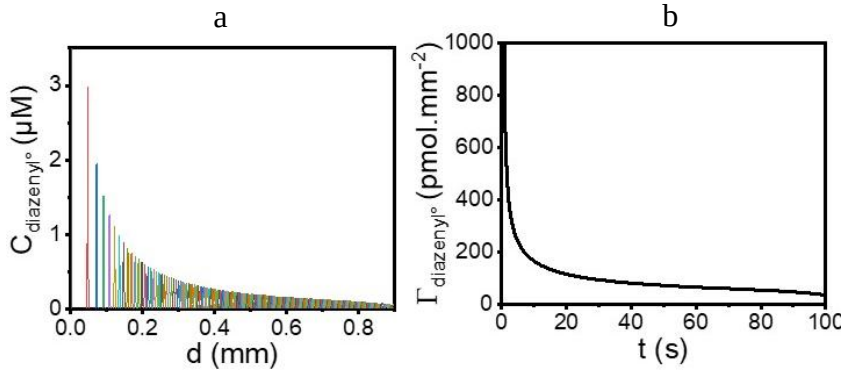

Figure S4: (a) Simulations of the concentration profiles of Diazenyl• plotted with the distance from the electrode at 0.1s time interval for R and b) the corresponding integration of the concentration profile over time $\Gamma_{Diazenyl}$•.

DFT simulated spectra

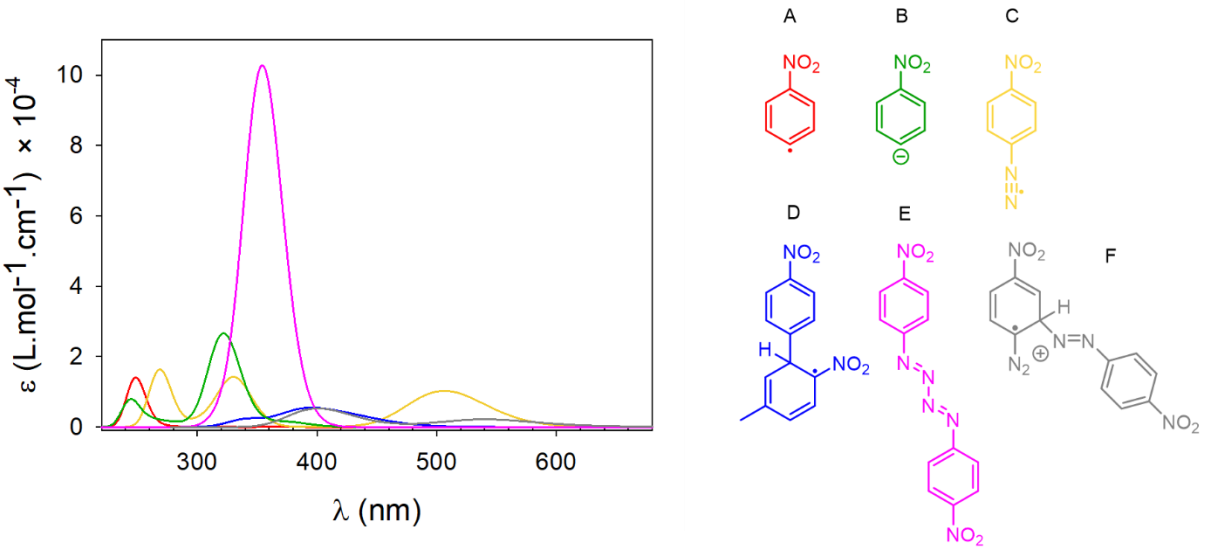

Figure S5. Simulated UV-Vis spectra for expected species obtained after reduction of the 4-nitrophenylbenzene diazonium.

Spectroelectrochemistry control experiments

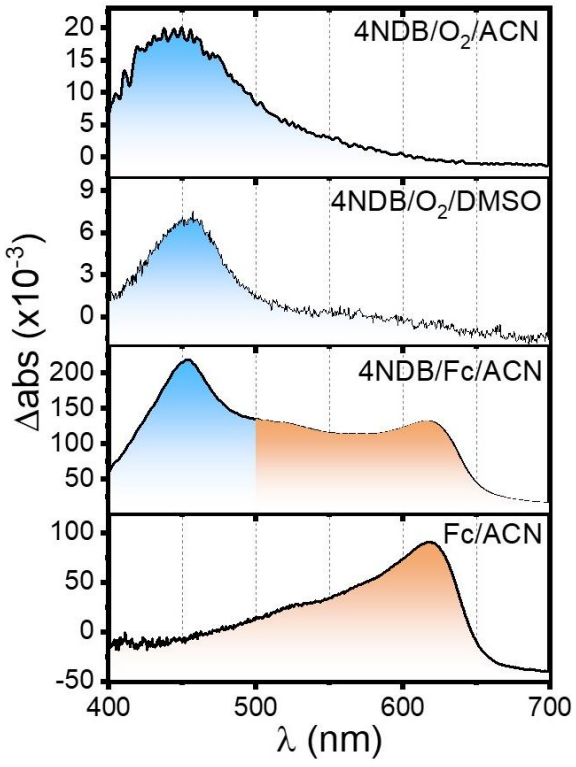

Figure S6. Absorption spectra recorded during spectroelectrochemical measurements of the mediated reduction of 4-NBD by $O_2^{\bullet-}$ a) in CH_3CN and b) in DMSO containing 1 mM of 4-NBD and 0.1M nBu_4PF_6. b) Recording of the chemical reduction of 1 mM 4-NDB by injection of 1 mM of ferrocene (Fc) in CH_3CN. d) Recording of the chemical oxidation of 1mM Fc by injection of 1 mM of $NOBF_4$ in CH_3CN.

Spectroelectrochemistry simulations for the secondary product coming from the diazenyl radical evolution

If the concentration of the product issued from the diazenyl decomposition (R) is considered in the simulation, a gradual accumulation of R within the diffusion layer of the electrode can be observed (Figure S7a). From those simulations one can observe an increase of Γ_R with time (Figure S7b). However, the simulation shows a continuous increase of R with time whereas experimentally maximum value of Δabs at each time, Δabs_{max}, a plateau is rapidely reached as shown in Figure 2c.

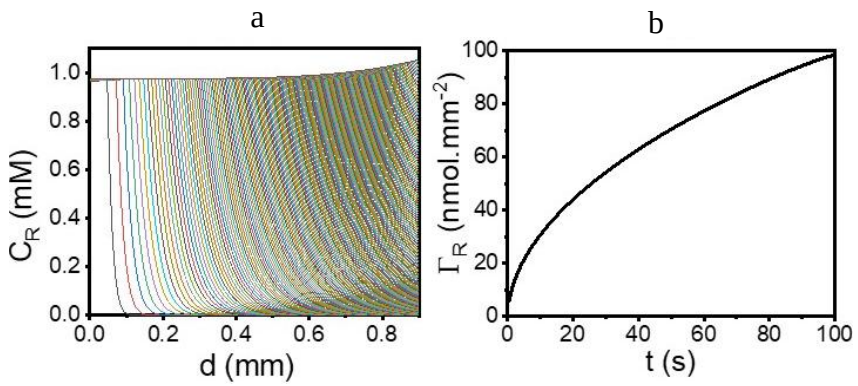

Figure S7. a) Simulations of the concentration profiles of R plotted with the distance from the electrode at 0.1s time interval and b) the corresponding integration of the concentration profile over time Γ_R also reported in Figure 2c.

This mechanism considered being insufficient to explain the experimental evolution of Δabs_{max} vs time, R was itself considered as an instable species in the model following a first order decomposition rate to give a secondary product with a decomposition rate constant $k_{d,R}$. The concentration profile of R with the distance from the electrode for various $k_{d,R}$ values are shown in Figure S8a and their corresponding Γ_R reported in Figure 2c are shown in Figure S8b.

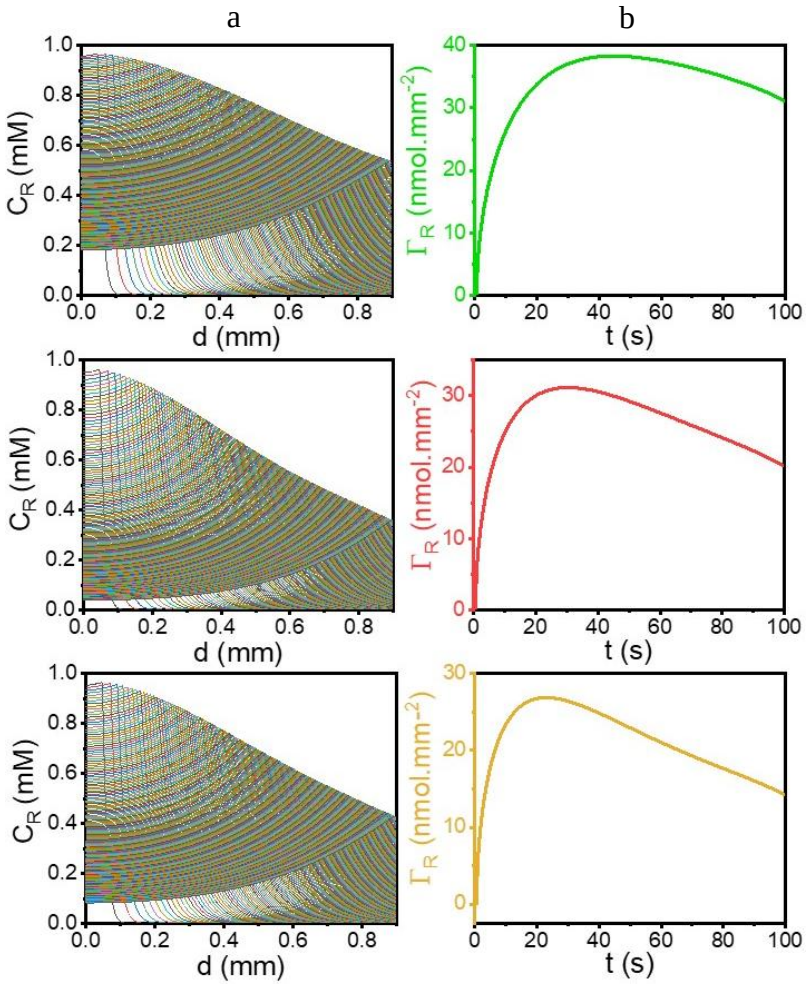

Figure S8. a) Simulations of the concentration profiles of R plotted with the distance from the electrode at 0.1s time interval and b) their corresponding Γ_R over time for the various $k_{d,R}$ values reported in Figure 2c.

Laser desorption ionisation (LDI) mass spectra

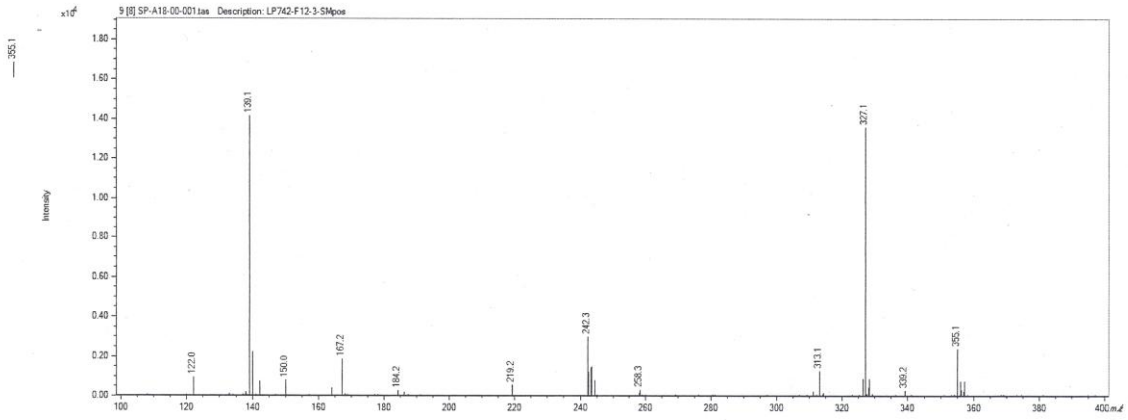

Figure S9. Mass spectrum of a purified fraction after electrolysis (see the radical scavengering part for details), recorded in Laser Desorption Ionisation (LDI) mode on a spiral-TOF JEOL JMS3000.

Computational details for UV-vis spectra simulation

UV-Vis calculation reports generated by quchemreport

Software Gaussian (2009+D.01)

Computational method DFT

Functional PBE1PBE

Basis set name 6-311+G(2d,2p)

Job type: Frequency and thermochemical analysis

Temperature 298.15 K

Job type: Time-dependent calculation

Number of calculated excited states and spin state 15

STRUCTURE: NO2Ph-radical

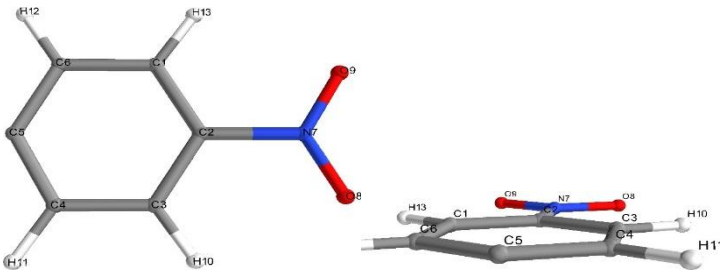

Formula C6H4NO2

Charge 0

Spin multiplicity 2

RESULTS

Total molecular energy -435.70748 hartrees

Unrestricted calculation	Alpha spin MO	Beta spin MO
HOMO number	32	31
LUMO+1 energies	-1.23 eV	-2.56 eV
LUMO energies	-2.68 eV	-2.74 eV
HOMO energies	-8.00 eV	-8.28 eV
HOMO-1 energies	-8.35 eV	-8.37 eV

Geometry optimization specific results

Converged nuclear repulsion energy 403.96183 Hartrees

Frequency and Thermochemistry specific results

Enthalpy at 298.15 K -435.60913 Hartrees

Gibbs free energy at 298.15 K -435.64928 Hartrees

Entropy at 298.15 K 0.00013 Hartrees

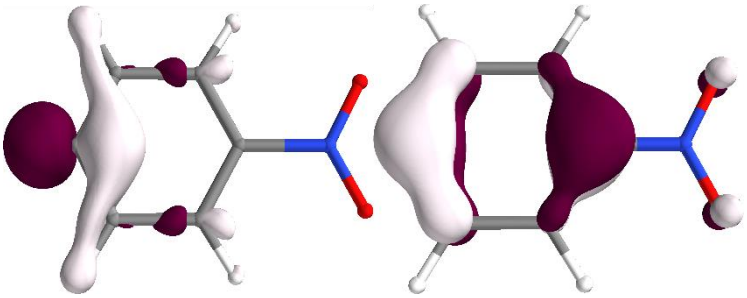

Representation of the HOMO of spin alpha (left) and spin beta (right).

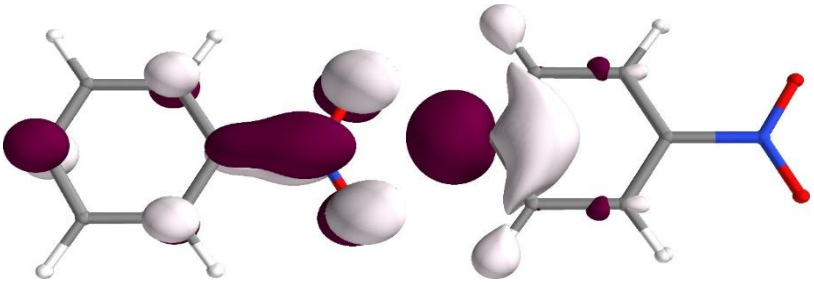

Representation of the LUMO of spin alpha (left) and spin beta (right).

Results concerning the calculated mono-electronic excitations.

E.S.	Symmetry	nm	cm^{-1}	*f*	R	Λ	d*CT*	q*CT*	Excitation description: initial OM - ending OM (% if > 5%)
1	3.468-A	422	23685	0.000	0.0	0.72	204.59	0.55	27a-33a (45) 27b-33b (43)
2	2.010-A	371	26905	0.001	-0.0	0.73	197.62	0.44	32a-33a (10) 31b-32b (83)
3	3.462-A	365	27352	0.000	-0.0	0.40	220.18	0.80	29a-33a (53) 29b-33b (40)
4	3.460-A	359	27823	0.000	0.0	0.74	134.39	0.38	30a-33a (33) 31a-34a (12) 30b-34b (12) 31b-33b (33)
5	3.383-A	316	31592	0.000	-0.0	0.51	106.57	0.69	28a-33a (50) 32a-33a (7) 28b-33b (36)
6	2.040-A	315	31724	0.000	0.0	0.52	262.88	0.74	30b-32b (98)
7	2.023-A	311	32123	0.000	0.1	0.38	236.23	0.81	29a-33a (40) 29b-33b (55)

8	2.171-A	307	32527	0.002	0.0	0.41	353.23	0.70	32a-33a (76) 31b-32b (11)
9	3.446-A	302	33046	0.001	-0.0	0.57	194.86	0.62	31a-33a (54) 30b-33b (31)
10	3.458-A	282	35456	0.002	-0.0	0.83	21.16	0.29	30a-33a (9) 31a-34a (36) 30b-34b (33) 31b-33b (18)
11	2.024-A	275	36269	0.001	-0.0	0.45	233.75	0.76	28a-33a (40) 28b-33b (55)
12	2.080-A	262	38121	0.010	0.0	0.54	274.60	0.69	31a-33a (31) 30b-33b (58) 31b-34b (7)
13	2.072-A	249	40131	0.000	-0.0	0.38	146.98	0.82	32a-34a (99)
14	2.035-A	248	40263	0.190	-0.1	0.63	282.64	0.63	30a-33a (50) 31b-33b (44)
15	3.432-A	246	40644	0.002	0.0	0.65	192.36	0.48	30a-34a (41) 31b-34b (52)

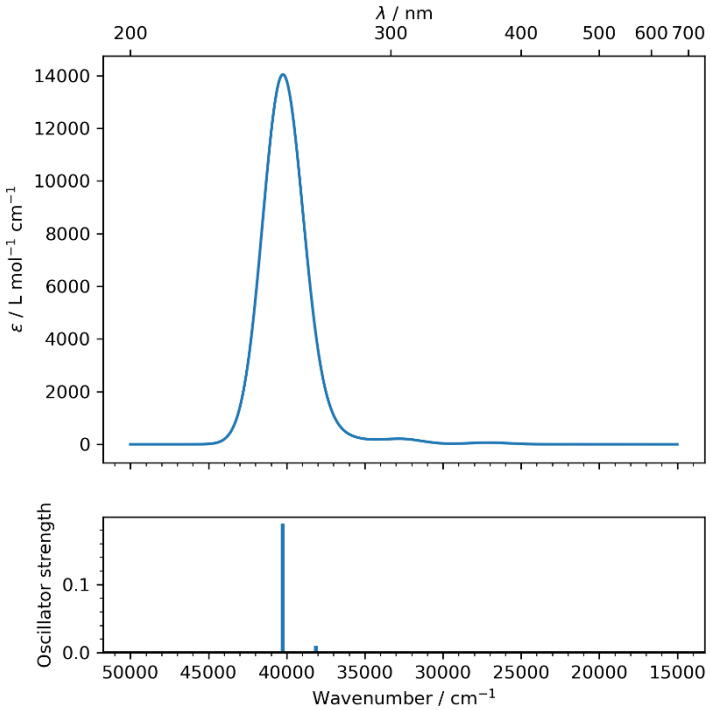

Calculated UV visible Absorption spectrum with a gaussian broadening (FWHM = 3000 cm-1)

Converged cartesian atomic coordinates in Angstroms

Atom	X	Y	Z
C	0.4830	-1.2185	-0.0002
C	-0.1794	0.0000	-0.0000
C	0.4830	1.2185	0.0001
C	1.8743	1.2230	0.0002
C	2.4927	-0.0000	0.0000
C	1.8743	-1.2230	-0.0001
N	-1.6458	0.0000	-0.0001
O	-2.2076	1.0776	-0.0003
O	-2.2076	-1.0776	0.0004
H	-0.0894	2.1355	0.0002
H	2.4269	2.1536	0.0004
H	2.4269	-2.1536	-0.0003
H	-0.0894	-2.1355	-0.0003

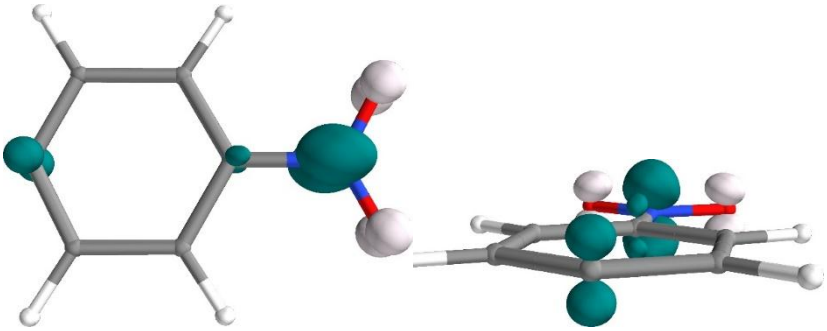

Representation of the Electron Density Difference (ES1-GS) from two points of view.

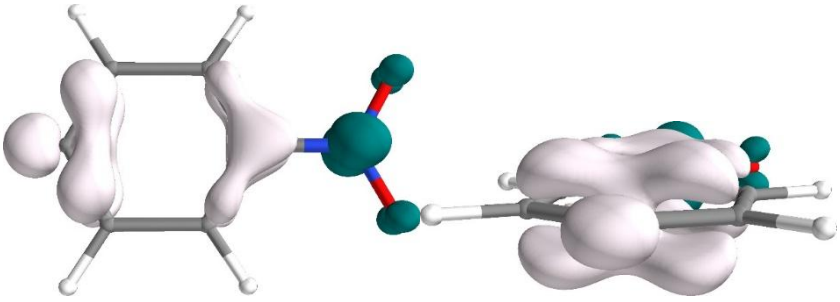

Representation of the Electron Density Difference (ES2-GS) from two points of view.

STRUCTURE: NO2Ph-anion

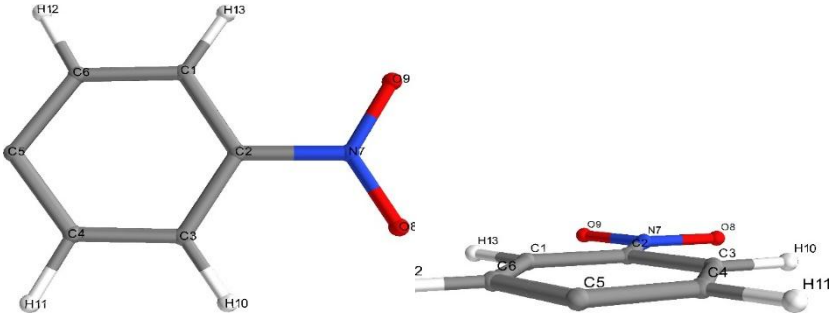

Chemical structure diagram with atomic numbering from two points of view.

Formula C6H4NO2-

Charge -1

Spin multiplicity 1

RESULTS

Total molecular energy	-435.77088 hartrees
HOMO number	32
LUMO+1 energies	3.59 eV
LUMO energies	1.56 eV
HOMO energies	-0.62 eV
HOMO-1 energies	-2.87 eV

Geometry optimization specific results

Converged nuclear repulsion energy 401.03888 Hartrees

Frequency and Thermochemistry specific results

Enthalpy at 298.15 K -435.67403 Hartrees

Gibbs free energy at 298.15 K -435.71358 Hartrees

Entropy at 298.15 K 0.00013 Hartrees

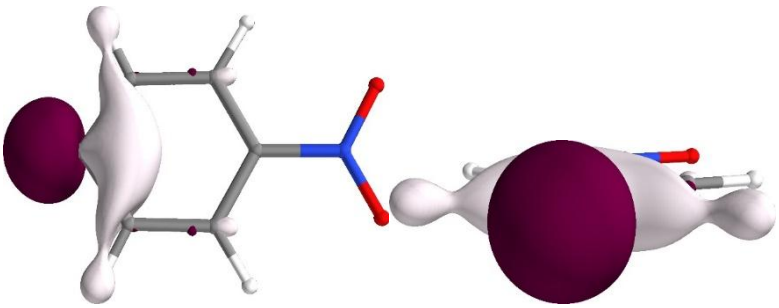

Representation of the HOMO from two points of view.

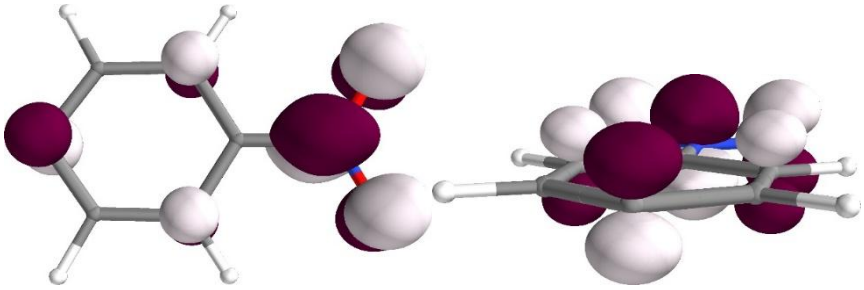

Representation of the LUMO from two points of view.

Results concerning the calculated mono-electronic excitations.

E.S.	Symmetry	nm	cm^{-1}	*f*	R	Λ	d*CT*	q*CT*	Excitation description: initial OM - ending OM (% if > 5%)
1	Singlet-A	1065	9385	0.001	0.0	0.31	444.31	0.86	32-33(99);
2	Singlet-A	419	23825	0.000	-0.0	0.34	186.90	0.83	32-36(99);
3	Singlet-A	374	26714	0.020	0.0	0.20	240.53	0.69	32-34(96);
4	Singlet-A	343	29130	0.008	-0.0	0.17	190.10	0.73	32-35(96);
5	Singlet-A	325	30759	0.010	0.0	0.45	261.64	0.78	30-33(98);
6	Singlet-A	321	31066	0.350	-0.2	0.55	302.38	0.66	31-33(86); 32-37(6);
7	Singlet-A	312	32029	0.000	0.2	0.46	137.56	0.74	29-33(97);
8	Singlet-A	306	32664	0.009	0.0	0.44	282.63	0.71	32-39(97);
9	Singlet-A	297	33587	0.007	0.0	0.21	291.30	0.63	31-33(7); 32-37(89);
10	Singlet-A	279	35839	0.015	-0.0	0.18	176.06	0.71	32-38(95);
11	Singlet-A	266	37476	0.001	-0.0	0.51	117.33	0.71	27-33(97);
12	Singlet-A	264	37774	0.009	-0.0	0.30	191.15	0.57	32-40(92);
13	Singlet-A	259	38520	0.018	0.0	0.21	233.54	0.58	32-41(95);
14	Singlet-A	244	40954	0.106	-0.0	0.27	194.99	0.48	32-42(96);
15	Singlet-A	230	43299	0.000	0.0	0.27	307.87	0.85	28-33(97);

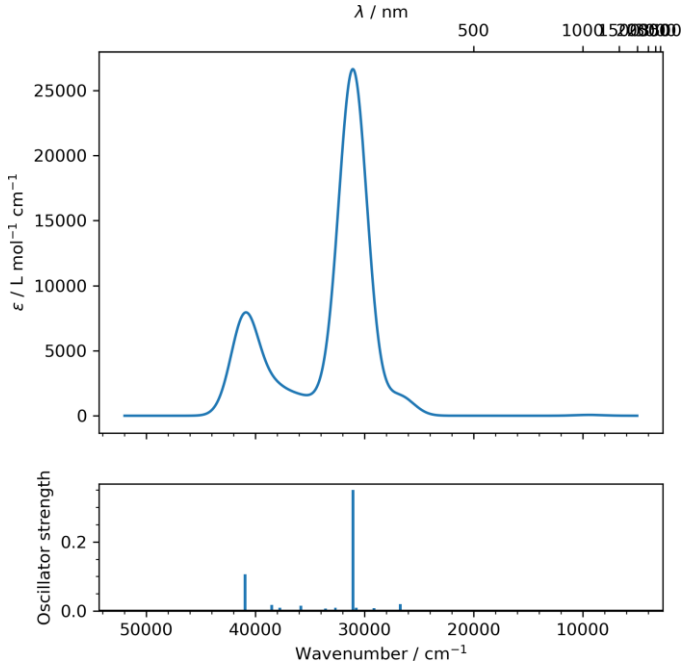

Calculated UV visible Absorption spectrum with a gaussian broadening (FWHM = 3000 cm-1)

Converged cartesian atomic coordinates in Angstroms

Atom	X	Y	Z
C	0.4815	-1.2079	0.0001
C	-0.2151	0.0000	0.0000
C	0.4815	1.2079	-0.0000
C	1.8673	1.1769	-0.0001
C	2.6588	-0.0000	-0.0000
C	1.8673	-1.1769	0.0001
N	-1.6493	0.0000	0.0000
O	-2.2426	1.0766	0.0001
O	-2.2425	-1.0766	-0.0002
H	-0.0785	2.1356	-0.0001
H	2.3676	2.1468	-0.0001
H	2.3675	-2.1468	0.0001
H	-0.0785	-2.1356	0.0001

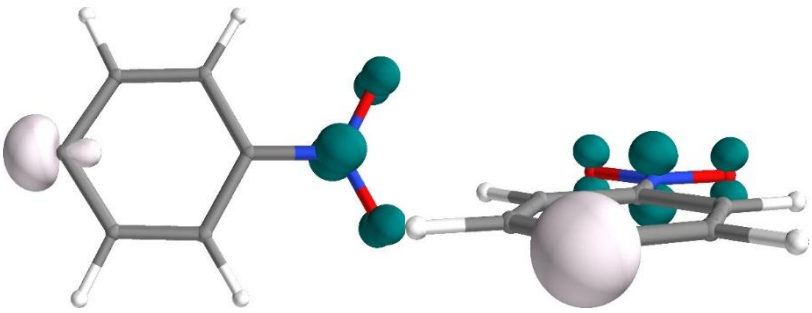

Representation of the Electron Density Difference (S1-S0) from two points of view.

STRUCTURE: paraNO2PhN2_radical

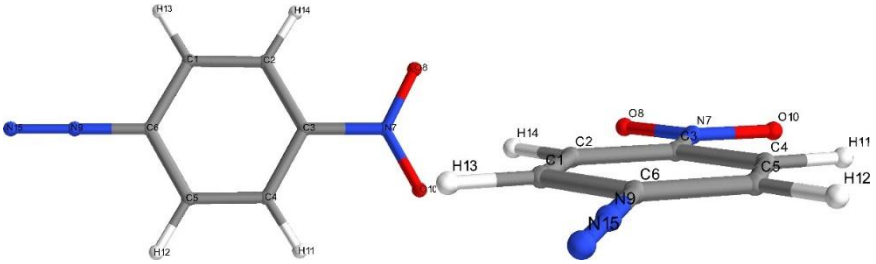

Chemical structure diagram with atomic numbering from two points of view.

Formula C6H4N3O2

Charge 0

Spin multiplicity 2

RESULTS

Unrestricted calculation	Alpha spin MO	Beta spin MO
HOMO number	39	38
Total molecular energy -545.13460 hartrees		
HOMO energies		
HOMO-1 energies		
LUMO+1 energies	-2.13 eV	-2.13 eV
LUMO energies	-2.35 eV	-3.16 eV

Geometry optimization specific results

Converged nuclear repulsion energy 548.73245 Hartrees

Frequency and Thermochemistry specific results

Enthalpy at 298.15 K -545.02476 Hartrees

Gibbs free energy at 298.15 K -545.07029 Hartrees

Entropy at 298.15 K 0.00015 Hartrees

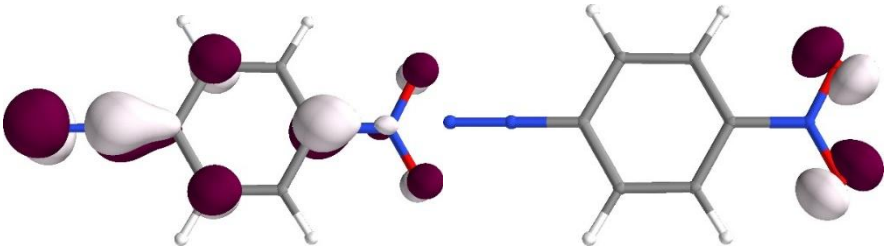

Representation of the HOMO of spin alpha (left) and spin beta (right).

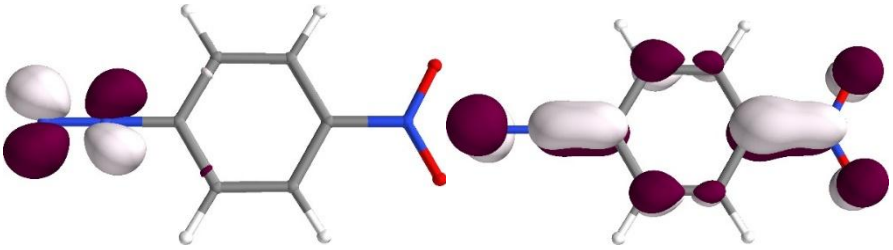

Representation of the LUMO of spin alpha (left) and spin beta (right).

Results concerning the calculated mono-electronic excitations.

E.S.	Symmetry	nm	cm^{-1}	*f*	R	Λ	d*CT*	q*CT*	Excitation description : initial OM - ending OM (% if > 5%)
1	2.046-A		1258	7947	0.000	0.0	0.50	282.68	0.73 39a-40a (96)
2	2.031-A	506	19744	0.142	-0.0	0.70	408.01	0.57	39a-41a (87) 37b-39b (11)
3	2.113-A	450	22187	0.001	0.0	0.48	151.55	0.70	39a-42a (93)
4	3.104-A	418	23868	0.001	0.0	0.65	284.66	0.55	34a-41a (25) 37a-41a (7) 35b-39b (28) 35b-41b (12) 36b-39b (17)
5	2.791-A	394	25333	0.000	0.0	0.43	243.10	0.77	38a-41a (7) 38b-39b (71) 38b-41b (18)
6	2.738-A	333	30013	0.000	0.0	0.46	237.63	0.75	36a-41a (6) 34b-39b (75) 34b-41b (16)
7	2.434-A	330	30224	0.191	0.0	0.72	80.72	0.32	39a-41a (7) 39a-44a (15) 36b-42b (11) 37b-39b (52)
8	2.203-A	307	32526	0.026	0.0	0.72	217.10	0.45	35b-39b (20) 36b-39b (71)
9	2.594-A	306	32646	0.000	-0.0	0.41	264.28	0.79	38a-41a (85) 38b-39b (8)
10	2.035-A	295	33826	0.006	-0.0	0.32	55.99	0.71	39a-43a (97)
11	2.749-A	278	35878	0.012	0.0	0.72	88.69	0.33	37a-42a (10) 39a-44a (53) 36b-42b (15) 37b-41b (7)
12	3.143-A	273	36519	0.000	-0.0	0.33	334.37	0.83	37b-40b (88)

13	2.821-A	268	37258	0.219	-0.0	0.71	29.96	0.27	37a-42a (22) 39a-44a (16) 36b-42b (16) 37b-39b (30)
14	2.637-A	267	37367	0.000	-0.0	0.45	259.47	0.76	36a-41a (86) 34b-39b (7)
15	2.046-A	250	39901	0.000	0.0	0.21	23.94	0.75	39a-45a (92)

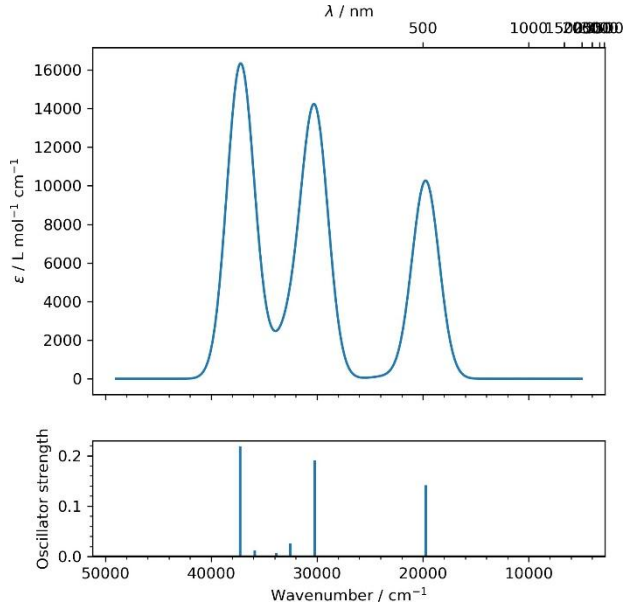

Calculated UV visible Absorption spectrum with a gaussian broadening (FWHM = 3000 cm-1)

Converged cartesian atomic coordinates in Angstroms

Atom	X	Y	Z
C	1.0435	-1.2346	0.0001
C	-0.3249	-1.2182	0.0001
C	-1.0100	-0.0000	0.0000
C	-0.3248	1.2182	0.0001
C	1.0435	1.2345	0.0001
C	1.7435	-0.0000	-0.0000
N	-2.4478	0.0000	-0.0000
O	-3.0175	-1.0821	-0.0001
N	3.0733	0.0000	0.0000
O	-3.0174	1.0822	-0.0001
H	-0.8926	2.1375	0.0001
H	1.5933	2.1651	0.0002
H	1.5932	-2.1652	0.0001
H	-0.8927	-2.1375	0.0001
N	4.2107	0.0000	- 0.0002

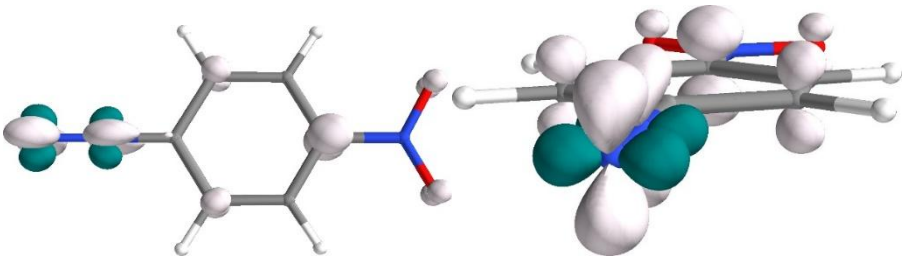

Representation of the Electron Density Difference (ES1-GS) from two points of view.

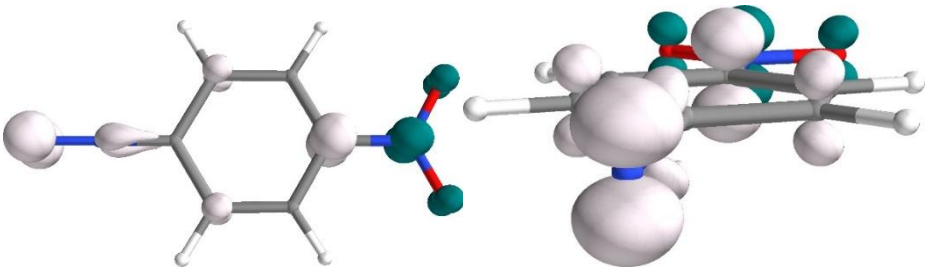

Representation of the Electron Density Difference (ES2-GS) from two points of view.

STRUCTURE: 4Me-2-4NO2Ph-NO2benzene_radical

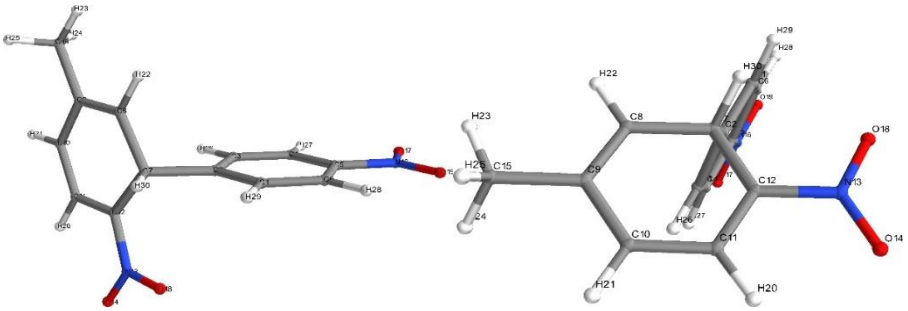

Chemical structure diagram with atomic numbering from two points of view.

Formula C13H11N2O4

Charge 0

Spin multiplicity 2

RESULTS

Total molecular energy -911.42760 hartrees

Unrestricted calculation	Alpha spin MO	Beta spin MO
HOMO number	68	67
LUMO+1 energies	-2.30 eV	-2.62 eV

LUMO energies	-2.65 eV	-3.78 eV
HOMO energies	-6.40 eV	-7.81 eV
HOMO-1 energies	-7.99 eV	-8.14 eV

Geometry optimization specific results

Converged nuclear repulsion energy 1371.58960 Hartrees

Frequency and Thermochemistry specific results

Enthalpy at 298.15 K -911.18601 Hartrees

Gibbs free energy at 298.15 K -911.24994 Hartrees

Entropy at 298.15 K 0.00021 Hartrees

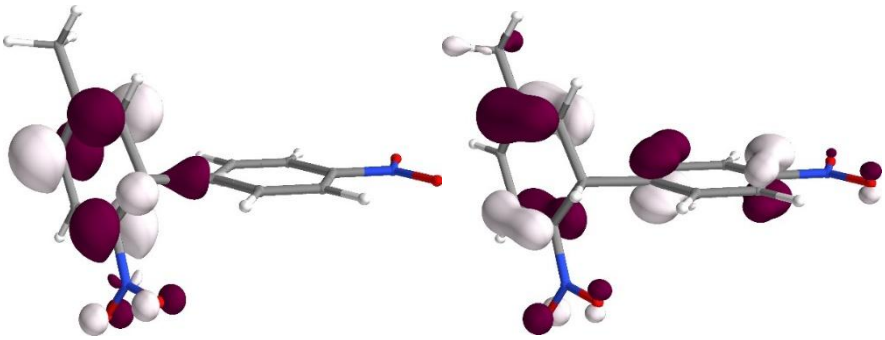

Representation of the HOMO of spin alpha (left) and spin beta (right).

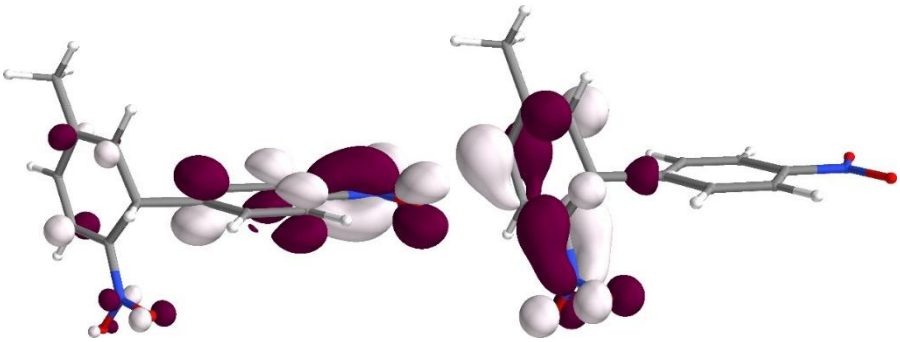

Representation of the LUMO of spin alpha (left) and spin beta (right).

Results concerning the calculated mono-electronic excitations.

E.S.	Symmetry	nm	cm−1	f	R	Λ	dCT	qCT	Excitation description : initial OM - ending OM (% if > 5%)
1	2.064-A	511	19555	0.001	2.8	0.60	296.44	0.45	68a-69a (14) 68a-70a (30) 65b-68b (7) 67b-

									68b (40)
2	2.805-A	452	22113	0.012	11.6	0.52	202.51	0.49	59a-70a (14) 68a-69a (9) 62b-68b (33) 62b-70b (8) 67b-68b (6)
3	2.579-A	440	22677	0.005	19.1	0.53	84.46	0.55	62b-68b (6) 64b-68b (44) 64b-70b (6) 65b-68b (16)
4	3.488-A	426	23466	0.000	-0.0	0.64	370.78	0.62	60a-69a (37) 59b-69b (41)
5	2.202-A	417	23924	0.035	1.1	0.44	356.31	0.50	68a-69a (41) 62b-68b (6) 64b-68b (10) 67b-68b (27)
6	2.252-A	392	25469	0.036	-6.5	0.50	294.94	0.55	68a-69a (24) 68a-70a (43) 67b-68b (12)
7	3.272-A	381	26204	0.001	1.8	0.53	462.48	0.47	67a-69a (23) 61b-68b (6) 65b-69b (7) 67b-69b (18)
8	2.469-A	377	26470	0.029	9.2	0.46	89.65	0.51	68a-70a (13) 61b-68b (27) 65b-68b (11) 66b-68b (17)
9	3.488-A	368	27145	0.000	-0.0	0.32	420.59	0.84	64a-69a (41) 63b-69b (44)
10	2.198-A	344	28997	0.002	3.3	0.50	172.94	0.63	61b-68b (16) 64b-68b (9) 66b-68b (65)
11	2.219-A	341	29325	0.028	-9.3	0.57	207.71	0.47	61b-68b (21) 64b-68b (9) 65b-68b (45)
12	3.185-A	322	31007	0.003	-5.6	0.51	193.89	0.36	66a-69a (7) 67a-70a (10) 58b-68b (6) 66b-69b (8) 67b-70b (14)
13	3.487-A	318	31391	0.000	-0.0	0.40	389.89	0.76	62a-69a (40) 60b-69b (43)
14	3.405-A	315	31668	0.000	-1.5	0.43	145.61	0.57	66a-69a (32) 66b-69b (28)
15	2.042-A	314	31807	0.000	-1.0	0.33	444.55	0.83	64a-69a (42) 63b-69b (46)

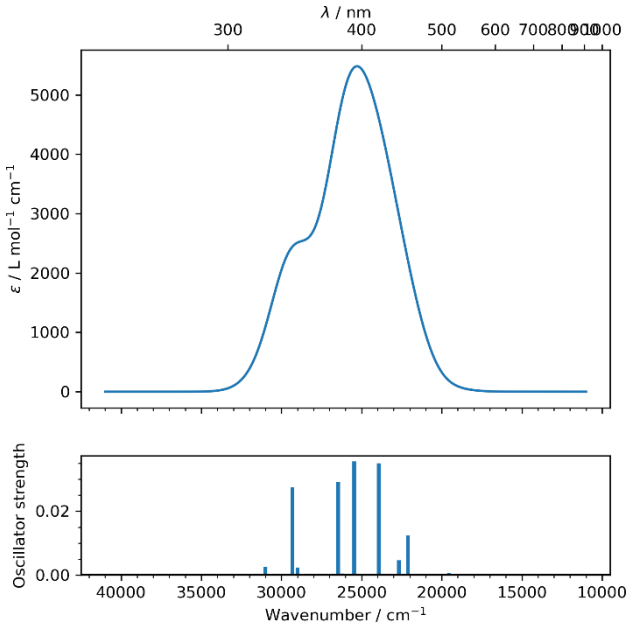

Calculated UV visible Absorption spectrum with a gaussian broadening (FWHM = 3000 cm-1)

Converged cartesian atomic coordinates in Angstroms

Atom	X	Y	Z
C	-1.1253	0.4119	1.4528
C	-0.1700	-0.0189	0.5396
C	-0.5798	-0.5596	-0.6769
C	-1.9240	-0.6708	-0.9821
C	-2.8533	-0.2403	-0.0499
C	-2.4751	0.3017	1.1657
C	1.3211	0.0626	0.8720
C	1.8857	-1.3215	0.9579
C	2.8792	-1.7916	0.1618
C	3.4638	-0.9211	-0.8024
C	3.0670	0.4110	-0.9070
C	2.0775	0.9001	-0.1013
N	1.7624	2.3002	-0.1487
O	2.2871	2.9917	-1.0082
C	3.3799	-3.1998	0.2716
N	-4.2795	-0.3627	-0.3609
O	-4.5805	-0.8419	-1.4370
O	0.9826	2.7168	0.6987
O	-5.0727	0.0201	0.4768
H	3.5457	1.0852	-1.6040
H	1.3861	0.5395	1.8587

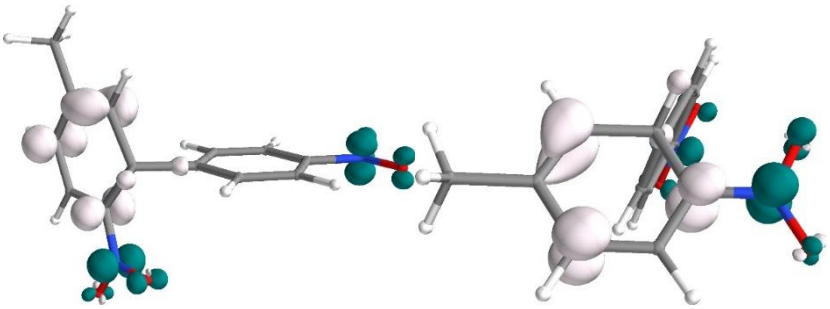

Representation of the Electron Density Difference (ES1-GS) from two points of view.

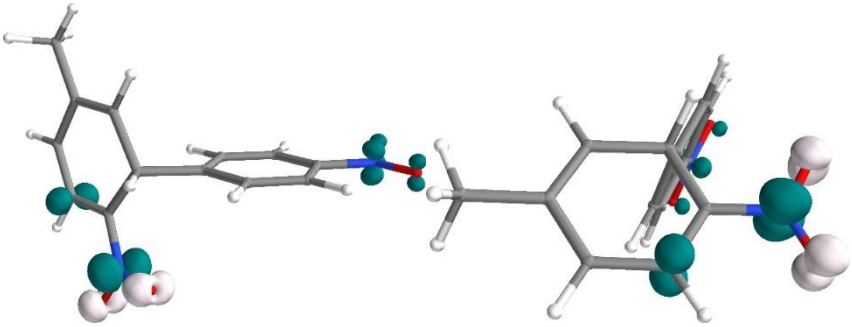

Representation of the Electron Density Difference (ES2-GS) from two points of view.

STRUCTURE: diNO2Ph_tetrazadiene

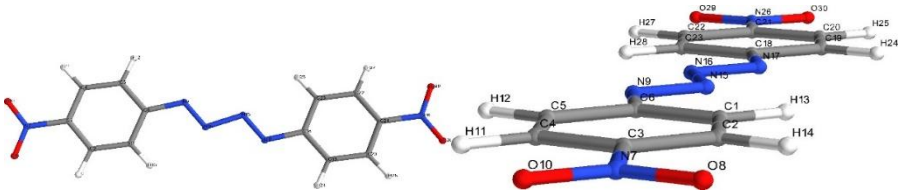

Chemical structure diagram with atomic numbering from two points of view.

Formula C12H8N6O4

Charge 0

Spin multiplicity 1

RESULTS

Total molecular energy	-1090.31828 hartrees
HOMO number	77
LUMO+1 energies	-2.99 eV
LUMO energies	-4.07 eV
HOMO energies	-7.63 eV
HOMO-1 energies	-8.08 eV

Geometry optimization specific results

Converged nuclear repulsion energy 1513.71786 Hartrees

Frequency and Thermochemistry specific results

Enthalpy at 298.15 K -1090.09352 Hartrees

Gibbs free energy at 298.15 K -1090.16352 Hartrees

Entropy at 298.15 K 0.00023 Hartrees

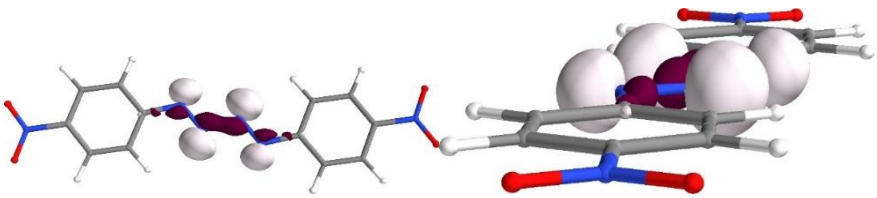

Representation of the HOMO from two points of view.

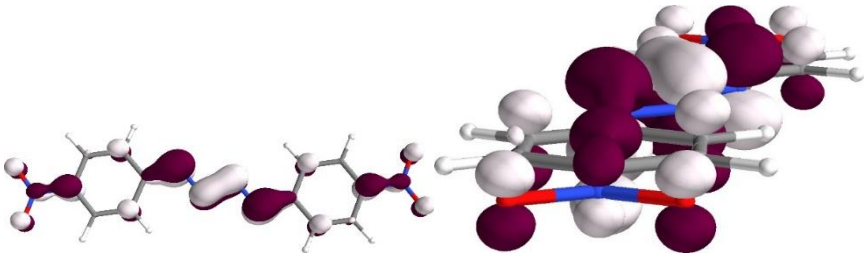

Representation of the LUMO from two points of view.

Most intense (> 50 km/mol) molecular vibrations in wavenumbers

Frequencies	Intensity	Symmetry
1683	289	A
1637	226	A
1627	84	A
1424	1073	A
1389	91	A
1243	61	A
1179	53	A
1136	79	A
899	69	A
870	157	A

Results concerning the calculated mono-electronic excitations.

E.S.	Symmetry	nm	cm^{-1}	*f*	R	Λ	d*CT*	q*CT*	Excitation description : initial OM - ending OM (% if > 5%)
1	Singlet-A	613	16289	0.000	0.0	0.47	0.01	0.74	77-78(94);
2	Singlet-A	395	25315	0.000	-0.4	0.51	0.05	0.68	73-78(83); 77-79(7);
3	Singlet-A	354	28208	1.405	0.6	0.77	0.04	0.49	76-78(98);
4	Singlet-A	334	29918	0.000	-0.2	0.30	0.04	0.80	73-78(10); 77-79(76);
5	Singlet-A	331	30122	0.000	0.0	0.34	0.07	0.78	70-79(26); 71-78(53); 71-80(13);
6	Singlet-A	331	30188	0.000	-0.0	0.38	0.05	0.75	70-78(51); 70-80(11); 71-79(27);
7	Singlet-A	327	30553	0.000	0.0	0.51	2.57	0.70	75-78(95);
8	Singlet-A	326	30625	0.075	-0.0	0.50	2.54	0.70	74-78(94);
9	Singlet-A	295	33891	0.000	-0.0	0.40	20.28	0.74	68-79(26); 69-78(55); 69-80(11);

10	Singlet-A	294	33948	0.000	0.0	0.40	20.31	0.76	68-78(57); 68-80(11); 69-79(27);
11	Singlet-A	288	34661	0.000	0.0	0.70	0.03	0.51	72-78(77); 76-79(20);
12	Singlet-A	277	36036	0.000	-0.0	0.33	0.98	0.79	77-80(87);
13	Singlet-A	268	37270	0.000	-0.0	0.65	0.00	0.50	72-78(19); 76-79(74);
14	Singlet-A	258	38656	0.000	0.0	0.32	0.03	0.72	71-78(10); 73-79(74);
15	Singlet-A	257	38771	0.000	-0.0	0.40	0.10	0.75	77-79(9); 77-81(75);

Converged cartesian atomic coordinates in Angstroms

Atom	X	Y	Z
C	3.2941	0.8902	-0.0002
C	4.6579	1.0936	-0.0001
C	5.5015	-0.0095	-0.0000
C	5.0266	-1.3086	-0.0001
C	3.6576	-1.5069	-0.0002
C	2.7925	-0.4152	-0.0002
N	6.9533	0.2122	0.0000
O	-7.6687	0.7694	-0.0005

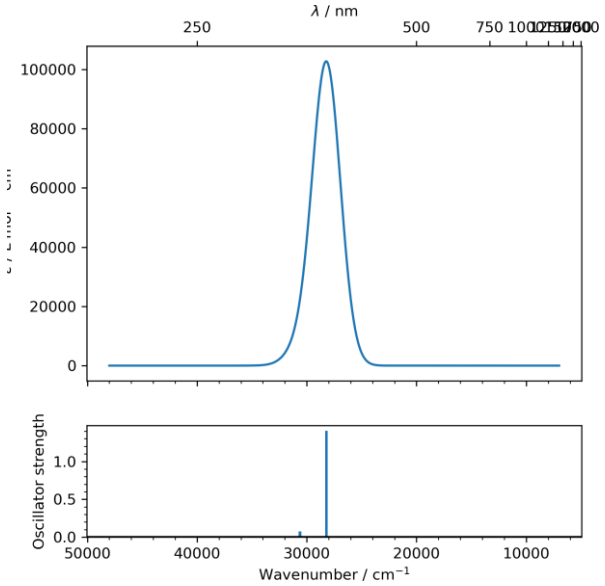

Calculated UV visible Absorption spectrum with a gaussian broadening (FWHM = 3000 cm-1)

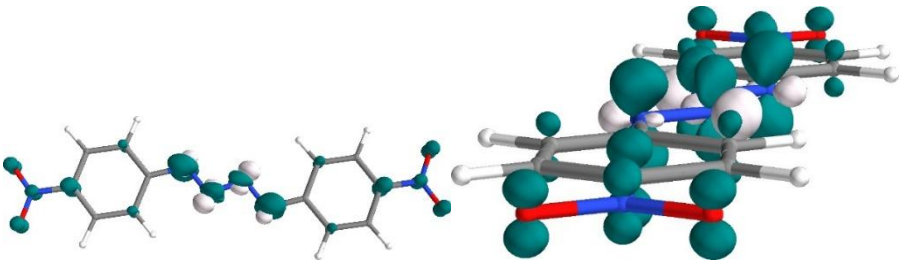

Representation of the Electron Density Difference (S1-S0) from two points of view.

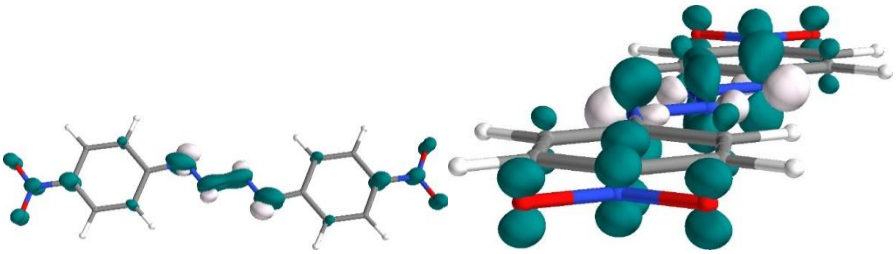

Representation of the Electron Density Difference (S2-S0) from two points of view.

STRUCTURE: ortho-coupling radical cation

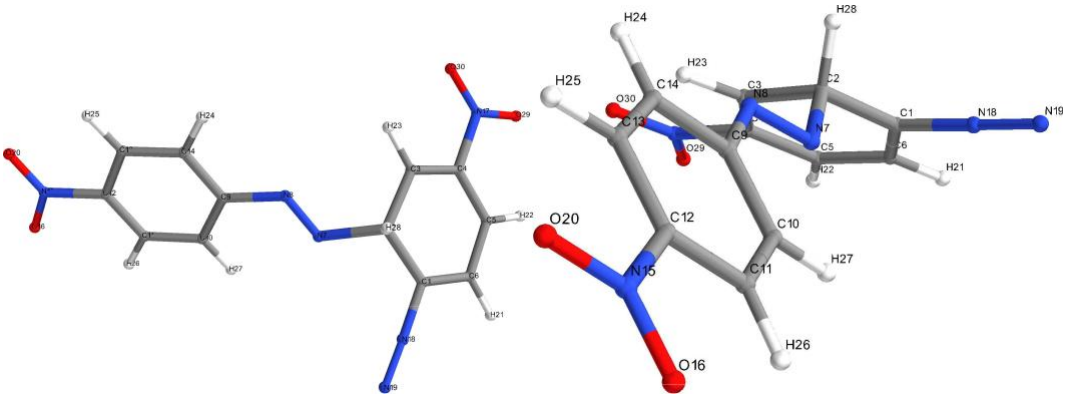

Chemical structure diagram with atomic numbering from two points of view.

Formula $C_{12}H_8N_6O_4^+$ Charge 1 Spin multiplicity 2

RESULTS

Total molecular energy	-1090.00415 hartrees	
Unrestricted calculation	Alpha spin MO	Beta spin MO

HOMO number	77	76
LUMO+1 energies	-7.12 eV	-7.02 eV
LUMO energies	-7.48 eV	-8.99 eV
HOMO energies	-11.12 eV	-11.23 eV
HOMO-1 energies	-11.24 eV	-11.24 eV
Geometry optimization specific results		
Converged nuclear repulsion energy	1603.18244 Hartrees	
Frequency and Thermochemistry specific results		
Enthalpy at 298.15 K	-1089.78107 Hartrees	
Gibbs free energy at 298.15 K	-1089.85253 Hartrees	
Entropy at 298.15 K	0.00024 Hartrees	

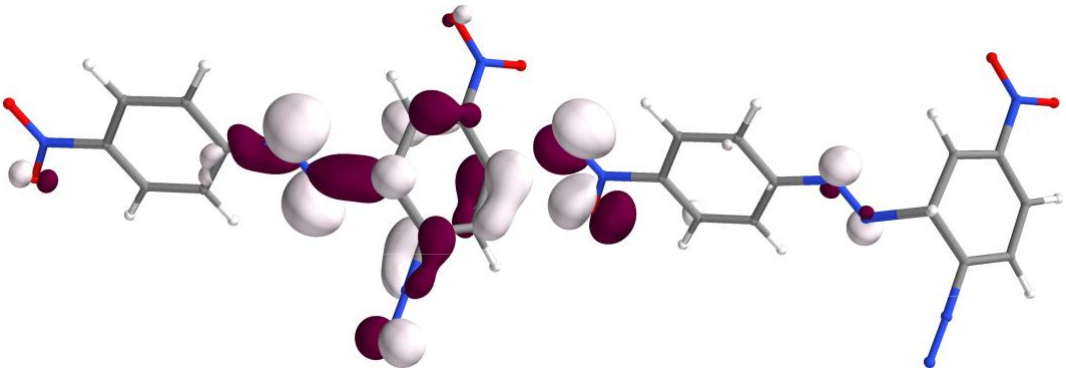

Representation of the HOMO of spin alpha (left) and spin beta (right).

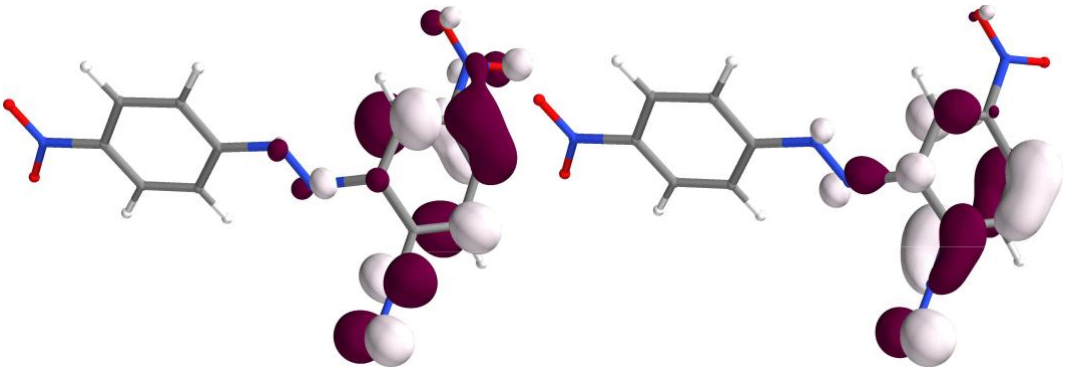

Representation of the LUMO of spin alpha (left) and spin beta (right).

E.S. Symmetry nm cm^{-1} f R Λ d_{CT} q_{CT} description : initial OM - ending OM (% if > 5%)

1	2.040-A	944	10588	0.045	-30.8	0.33	617.57	0.84	73b-77b (45) 74b-77b (29) 76b-77b (20)
2	2.035-A	781	12793	0.001	-4.3	0.29	579.30	0.85	73b-77b (34) 74b-77b (46) 75b-77b (17)
3	2.034-A	744	13439	0.000	-0.5	0.11	639.30	0.92	73b-77b (9) 74b-77b (6) 75b-77b (80)
4	2.035-A	663	15081	0.001	-0.2	0.23	802.67	0.90	73b-77b (6) 74b-77b (16) 76b-77b (75)
5	3.316-A	597	16747	0.002	-5.9	0.51	27.71	0.47	71a-80a (14) 77a-78a (8) 77a-80a (25) 73b-80b (11) 74b-80b (9)
7	2.136-A	540	18494	0.029	-50.7	0.61	323.62	0.43	71a-78a (9) 77a-78a (57) 67b-77b (16)
15	2.187-A	428	23324	0.018	-61.4	0.57	231.98	0.36	71a-78a (12) 77a-78a (14) 77a-80a (8) 67b-77b (29) 73b-80b (8)
16	2.596-A	409	24446	0.021	31.3	0.48	212.88	0.38	71a-80a (6) 77a-78a (10) 77a-80a (22) 67b-77b (11)
19	3.049-A	393	25382	0.026	-13.4	0.44	450.33	0.52	71a-78a (20) 74a-78a (19) 67b-77b (10) 68b-77b (7) 73b-79b (7)
21	2.969-A	387	25791	0.013	11.7	0.32	498.42	0.72	71a-78a (6) 74a-78a (49) 76a-78a (9)

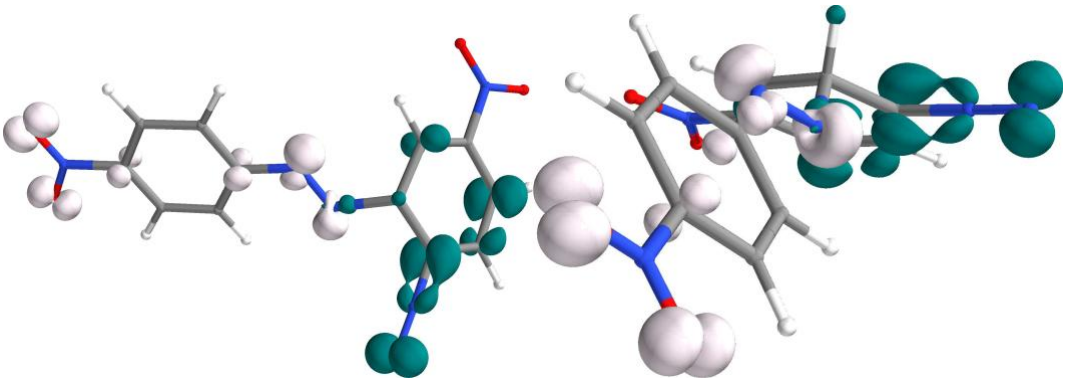

Representation of the Electron Density Difference (ES1-GS) from two points of view.

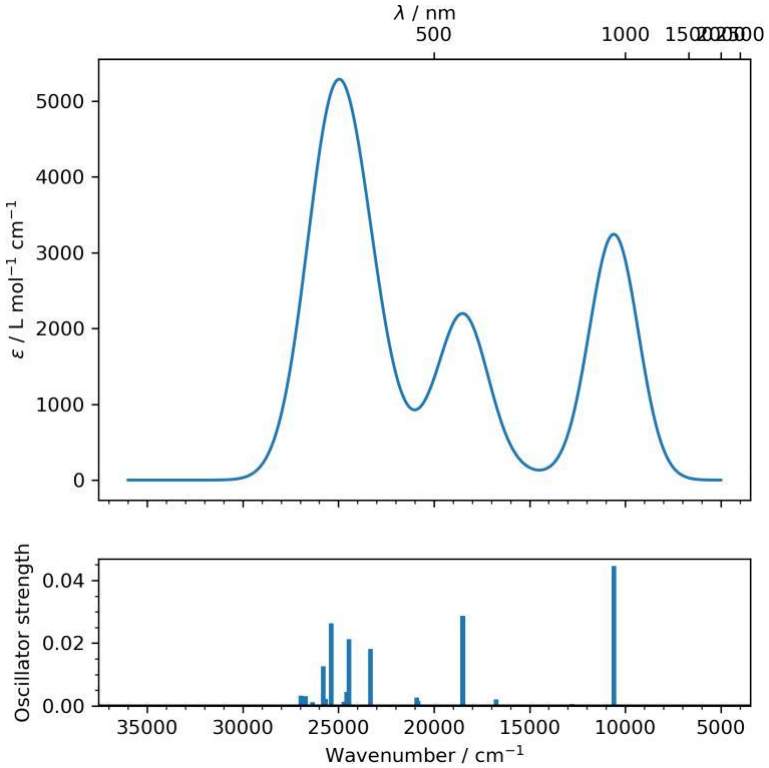

Calculated UV visible Absorption spectrum with a gaussian broadening (FWHM = 3000 cm^{-1})

Converged cartesian atomic coordinates in Angstroms

Atom	X	Y	Z
C	-2.7438	1.7635	0.1630
C	-1.9170	0.6931	0.7940
C	-2.5074	-0.6415	0.5826
C	-3.6433	-0.8140	-0.1266
C	-4.3700	0.2485	-0.7059
C	-3.9091	1.5444	-0.5573
N	-0.4869	0.7663	0.2472
N	0.2512	-0.0107	0.8432
C	1.6064	-0.0467	0.4565
C	2.1280	0.6722	-0.6230
C	3.4710	0.5661	-0.9122
C	4.2635	-0.2526	-0.1177
C	3.7651	-0.9739	0.9502
C	2.4147	-0.8705	1.2360
N	5.7024	-0.3589	-0.4335
O	6.1035	0.2813	-1.3808
N	-4.1582	-2.1914	-0.3173
N	-2.2800	3.0198	0.2730
N	-1.8652	4.0448	0.3822
O	6.3685	-1.0762	0.2792
H	-4.4454	2.3749	-0.9979
H	-5.2693	0.0320	-1.2662
H	-1.9790	-1.4958	0.9875
H	1.9739	-1.4178	2.0586

H	4.4286	-1.5981	1.5312
H	3.9223	1.0979	-1.7378
H	1.4821	1.2951	-1.2260
H	-1.8099	0.8752	1.8711
O	-5.1910	-2.2913	-0.9383
O	-3.5054	-3.0870	0.1622

References

1 Y. Wang, E. I. Rogers and R. G. Compton, *Journal of Electroanalytical Chemistry*, 2010, **648**, 15–19.

2 C. Amatore, C. Lefrou and F. Pflüger, *Journal of Electroanalytical Chemistry and Interfacial Electrochemistry*, 1989, **270**, 43–59.

3 O. Alévêque, E. Levillain and L. Sanguinet, *Electrochemistry Communications*, 2015, **51**, 108–112.

4 *M. J. Frisch, G. W. Trucks, H. B. Schlegel, G. E. Scuseria, M. A. Robb, J. R. Cheeseman, G. Scalmani, V. Barone, B. Mennucci, G. A. Petersson, H. Nakatsuji, M. Caricato, X. Li, H. P. Hratchian, A. F. Izmaylov, J. Bloino, G. Zheng, J. L. Sonnenberg, M. Hada, M. Ehara et al., Gaussian ~09 Revision D.01.*

5 C. Adamo and V. Barone, *The Journal of Chemical Physics*, 1999, **110**, 6158–6170.

6 T. Cauchy and B. Da Mota, *University of Angers, 2020*.

7 G. M. Sheldrick, *Acta Crystallographica Section A*, 2015, **71**, 3–8.

8 G. M. Sheldrick, *Acta Crystallographica Section C*, 2015, **71**, 3–8.

9 L. J. Farrugia, *J Appl Crystallogr*, 2012, **45**, 849–854.

10 V. Shkirskiy, J. Billon, E. Levillain and C. Gautier, *Langmuir*, 2021, **37**, 12834–12841.

11 Q. Li, C. Batchelor-McAuley, N. S. Lawrence, R. S. Hartshorne and R. G. Compton, *Journal of Electroanalytical Chemistry*, 2013, **688**, 328–335.